INTERNATIONAL JOURNAL FOR NUMERICAL METHODS IN FLUIDS
Int. J. Numer. Meth. Fluids 2006; **52**:163–197
Published online 10 February 2006 in Wiley InterScience (www.interscience.wiley.com). DOI: 10.1002/fld.1173

Analytic study of 2D and 3D grid motion using modified Laplacian

Clarence Burg*,†,‡

Department of Mathematics, University of Central Arkansas, Conway, AR 72035, U.S.A.

SUMMARY

The modified Laplacian has been used to move unstructured grids in response to changes in the surface grid for a variety of grid movement applications including store separation, aero-elastic wing deformation and free surface flow simulations. However, the use of the modified Laplacian can result in elements with negative areas/volumes, because it has no inherent mechanism to prevent inversion of elements. In this paper, the use of a modified Laplacian is studied analytically for a two-dimensional problem of deforming the inner circle of two concentric circles and for a three-dimensional problem of deforming the inner sphere of two concentric spheres. By analysing the exact solution for this problem, the amount of translation and deformation of the inner circle that maintains a valid mesh is determined. A general grid movement theorem is presented which determines analytically the maximum allowable deformation before an invalid mesh results. Under certain circumstances, the inner circle and sphere can be expanded until it reaches the outer circle or sphere, while remaining a valid grid, and the inner circle and sphere can be rotated by an extreme amount before failure of the mesh occurs. By choosing the exponent to the modified Laplacian appropriately, extreme deformations for single frequency deformations is possible, although for practical applications where the grid movement has multiple frequencies, choosing the optimal exponent for the modified Laplacian may not be practical or provide much improvement. For grid movement simulations involving rigid body translation and rotation or uniform expansion, the modified Laplacian can yield excellent results, and the optimum choice of the modified Laplacian can be analytically determined for these types of motions, but when there are multiple frequencies in the deformation, the modified Laplacian does not allow much deformation before an invalid grid results.

KEY WORDS: unstructured grids; grid movement; modified Laplacian; linear spring analogy

1. PROBLEM DEFINITION

The two-dimensional domain consists of two concentric circles. The inner circle has a radius of 1 unit and the outer circle has a radius of R, which is greater than 1, as is shown in

*Correspondence to: C. Burg, Department of Mathematics, UCA Box 4912, 201 Donaghey Ave., University of Central Arkansas, Conway, AR 72035, U.S.A.
†E-mail: clarenceb@uca.edu
‡Visiting Assistant Professor.

Received 26 August 2004
Revised 15 November 2005
Accepted 16 November 2005

Figure 1. The inner circle is deformed by a scalar $d(\theta)$, while the outer circle is fixed. The 3D domain similarly consists of 2 concentric spheres, where the inner sphere is deformed by a scalar $d(\theta, \phi)$. The use of the modified Laplacian for grid movement applications provides a scalar solution which represents an amount of deformation, but the interpretation of this deformation is problem dependent. The deformation can represent a translation in the x- or y-directions, a growth or contraction of the inner circle in the radial direction, or a rotation. In each case, the deformation within the interior of the domain is determined from the boundary definition and the choice of modification to the Laplacian. If the inner circle is to be translated by a constant amount A in the x-direction or if the radius of the inner circle is to increase by a constant amount A, the solution of this Laplacian will be the same for these two cases, because the boundary definition of a displacement value of A is the same. However, the interpretation of the result is different.

The Laplacian is being studied in this report, as well as a modified Laplacian. In particular, since this is a radial symmetric problem, the modified Laplacian includes a factor of r raised to some exponent, or

$$\nabla \cdot (r^q \nabla d) = 0 \tag{1}$$

If $q = 0$, then the traditional Laplacian is recovered. Converting this equation to polar coordinates in 2D, the modified Laplacian can be written as

$$\frac{1}{r} \frac{\partial}{\partial r} \left(r^{q+1} \frac{\partial d}{\partial r} \right) + r^{q-2} \frac{\partial^2 d}{\partial \theta^2} = 0 \tag{2}$$

and to spherical coordinates in 3D, the modified Laplacian can be written as

$$\nabla \cdot (r^q \nabla d) = \frac{1}{r^2} \frac{\partial}{\partial r} \left(r^{q+2} \frac{\partial d}{\partial r} \right) + \frac{r^{q-2}}{\sin \theta} \frac{\partial}{\partial \theta} \left(\sin \theta \frac{\partial d}{\partial \theta} \right) + \frac{r^{q-2}}{\sin^2 \theta} \frac{\partial^2 d}{\partial \phi^2} = 0 \tag{3}$$

The solution of the Laplacian will consist of a radial component and a series of solutions based on a frequency decomposition. In order to determine the maximum allowable deformation, a

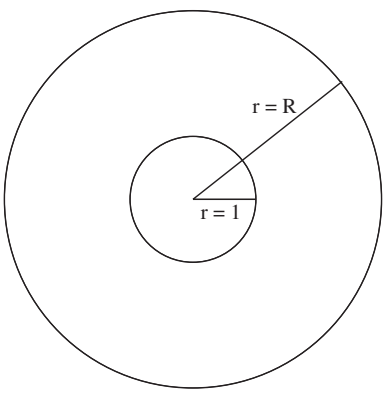

Figure 1. Two concentric circles with radii of 1 and R.

theorem is needed to determine analytically when the deformation in the grid results in an invalid mesh. This theorem deals with the gradient of the solution to the Laplacian dotted into the direction of the deformation. Only two deformation directions will be considered, since these are the limiting cases—deformation in the radial direction only and deformation in the rotational direction only. Translations can be viewed as a combination of a radial component and a rotational component.

In the next section, a brief review of grid movement algorithms is given, followed by a general grid movement theorem that defines the limitations of grid movement. Then, the 2D Laplacian is studied in regards to determining the limitations of grid movement, followed by an analysis of the 2D modified Laplacian and the 3D modified Laplacian. Computational verification is performed on the 2D case, where the behaviour of the modified Laplacian for single frequency deformations is studied. Finally, a brief presentation of the similarities between the modified Laplacian and the linear spring analogy for a perfect grid between two concentric circles is given, and the modified Laplacian is compared with a variant of the Laplacian used in a space–time/finite-element flow solver.

2. OVERVIEW OF GRID MOVEMENT ALGORITHMS

The motion of grids is required for several different types of computational simulations, including aero-elastic motion of wings and other deformable surfaces acted upon by external or internal forces, motion of objects moving relative to one another such as for storage separation simulations, deformation of movable interfaces between immiscible fluids, such as the water/air interface for simulation of flow past ships, and shape-based design optimization, where the shape of the object changes with the goal of optimizing some performance criterion. In each of these cases, the motion of the grid differs significantly. For instance, when two objects are moving relative to each other, the surface of the objects are typically not deforming, and the motions can be considered as rotations and translations. For aero-elastic motion of wings, the surfaces deform, and the interior grid must be moved to match the surfaces, but surface to surface interactions may not exist. For water/air interface simulations around ships, the water/air interface changes shape, and the intersection of this interface with the ship's hull changes along with the interior grid. The motion of the aero-elastic wings and of the water/air interface simulations, along with the shape-based numerical design optimization, involve more motions than just translation and rotation, because of the higher frequency components of the motion. These higher frequency components severely restrict the application of certain grid movement strategies, including the use of the Laplacian and modified Laplacian.

The various grid movement strategies can be classified into six general categories:

1. Algebraic transformations.
2. Trans-finite interpolation.
3. The Laplacian and modified Laplacian.
4. The linear elasticity equations.
5. The linear spring analogy.
6. The torsional spring analogy.

For some types of applications, algebraic transformations are quite acceptable. For instance, if the effects of small changes in the shape of an isolated wing are being studied, where the

changes are given by an algebraic function, then the deformation of the wing's surface as well as the grid in the computational domain can be applied via an algebraic transformation.

Trans-finite interpolation, or TFI, is widely used within structured grids to interpolate the surface deformations into a structured grid. This methodology is computationally efficient, easy to code and highly effective, but it cannot be directly applied to unstructured grids without significantly altering the generality afforded by unstructured grids.

The Laplacian and modified Laplacian have been used to propagate surface deformations within the interior grid. Lohner [1] used a modified Laplacian to propagate the deformations on the air/water interface into the volume grid where the stiffness coefficient varied with the distance from the viscous surfaces, which is similar to the modified Laplacian with $q = -1$. Crumpton and Giles [2] used a modified Laplacian where the stiffness was inversely proportional to the cell area/volume. Their choice for the stiffness is roughly equivalent to a value of $q = -2$ in 2D and $q = -3$ in 3D. Masud and Hughes [3] used a variant of the Laplacian, which will be analysed in detail in a later section, and is shown to be more restrictive than the optimal modified Laplacian.

The linear elasticity equations, which are a superset of the Laplacian, are gaining wider acceptance as a robust grid movement strategy [4–6]. The linear elasticity equations are

$$\nabla \cdot (\lambda \operatorname{tr}(\varepsilon(\mathbf{d}))I + 2\mu\varepsilon(\mathbf{d})) = 0 \tag{4}$$

where $\mathbf{d}$ is the displacement vector, tr( ) is the trace operator, λ and μ are the Lamé constants, I is the identity tensor, and $\varepsilon(\mathbf{d})$ is the strain tensor given by

$$\varepsilon(\mathbf{d}) = \tfrac{1}{2}(\nabla\mathbf{d} + (\nabla\mathbf{d})^{\mathrm{T}}) \tag{5}$$

with appropriate displacement boundary conditions. These equations represent a vector-valued set of equations, so that the solution $\mathbf{d}$ is a vector, and represents both a propagation amount and a propagation direction. (For the Laplacian, the displacement is a scalar—the direction must be supplied.) However, for successful grid movement, the Lamé constants within the elasticity equations must be chosen appropriately. In Tezduyar *et al.* [7] mesh deformation based on changes in the shape and volume of each element is accomplished by altering the ratio of these two coefficients. Additional investigations of the linear elasticity equations are described in Stein *et al.* [8].

If $\lambda = 1$ and $\mu = 0$, then the linear elasticity equations reduce to a set of decoupled Laplacian equations with a different equation for each direction. Thus, the Laplacian is a subset of the linear elasticity equations. This comparison also demonstrates that the Laplacian can be solved for the deformation in each separate direction, in which case the deformation direction is implied.

The linear spring analogy was first proposed by Batina [9], where the edges of the unstructured grid are replaced by linear springs whose stiffness is inversely proportional to the length of the edges and the nodes are allowed to move in response to the forces applied to the surface. This grid movement strategy is computationally efficient, being solved with a small number of passes through the nodes. However, the original linear spring analogy is not a robust strategy for extreme mesh movement, because it has no mechanism to prevent inverted elements, where the area/volume is negative. Due to the ease of implementation and the computational efficiency of this approach, several researchers have developed modifications to the linear spring approach to improve the robustness of the algorithm, including Anderson [10], Singh *et al.* [11], Zhang and Belegundu [12], and Samareh [13].

Finally, the torsional spring analogy was developed by Nakahashi and Deiwert [14] and was used by Farhat *et al.* [15], where the linear spring system is augmented with torsional springs in each corner, whose stiffness is inversely proportional to the sine of the angle. Using this approach, extreme mesh deformation in 2D unstructured grids was demonstrated, without generating inverted elements. Degand and Farhat [16] extended the torsional spring analogy to 3D by decomposing each 3D element in a set of 2D cuts and applied the 2D torsional spring approach to these cuts. Murayama *et al.* [17] extended the torsional spring approach to 3D by simply adding the torsional spring stiffness coefficients to the edge stiffness coefficients, and demonstrated extreme distortions on a 3D cube within a cube. Burg [18] has also extended the 2D torsional spring analogy to 3D by developing a new derivation of the 2D torsional springs which readily extends to 3D. His algorithm has been used for viscous water/air interface simulations about surface ships [19, 20].

3. GENERAL GRID MOVEMENT THEOREM

Grid movement algorithms fail due to the generation of elements with negative areas and volumes. The generation of these bad elements is caused when nodes pass other nodes or edges. In other words, they are caused when a node moves further than its neighbours, so that it overcomes the distance between the node and its neighbours.

Definitions
A *valid grid* is a mapping $\psi(\mathbf{x})$ from Ω_1 to $\Omega_2 = \{\mathbf{y}|\mathbf{y} = \psi(\mathbf{x}) \forall \mathbf{x} \in \Omega_1\}$, such that $\psi(\mathbf{x}_2) = \psi(\mathbf{x}_1)$ if and only if $\mathbf{x}_2 = \mathbf{x}_1$. A *deformed grid* includes the mapping $\psi(\mathbf{x})$, a deformation amount $P(\psi(\mathbf{x}))$ and a deformation direction $\mathbf{s}$ with $\|\mathbf{s}\| = 1$ and is a mapping from Ω_1 to $\Omega_P = \{\mathbf{y}|\mathbf{y} = \psi(\mathbf{x}) + \mathbf{s}P(\psi(\mathbf{x}))\forall \mathbf{x} \in \Omega_1\}$.

Theorem
A deformed grid is a valid grid if and only if $\nabla P(\psi(\mathbf{x})) \cdot \mathbf{s} \neq -1$ for all $\mathbf{x} \in \Omega_1$, where P is the deformation amount and $\mathbf{s}$ is the deformation direction, with $\|\mathbf{s}\| = 1$.

Proof
Given any point $\mathbf{x} \in \Omega_1$ and a deformation direction $\mathbf{s}$, restrict y to the space such that $\psi(\mathbf{y}) = \psi(\mathbf{x}) + t\mathbf{s}$. Assume the deformed grid is valid, so that $\psi(\mathbf{x}) + \mathbf{s}P(\psi(\mathbf{x})) = \psi(\mathbf{y}) + \mathbf{s}P(\psi(\mathbf{y}))$ if and only if $\mathbf{x} = \mathbf{y}$. Hence, $\mathbf{x} \neq \mathbf{y}$ if and only if $\psi(\mathbf{x}) + \mathbf{s}P(\psi(\mathbf{x})) \neq \psi(\mathbf{y}) + \mathbf{s}P(\psi(\mathbf{y}))$. Subtracting $\psi(\mathbf{x})$ from both sides and dotting into $\mathbf{s}$ yields

$$\begin{aligned}
(\psi(\mathbf{x}) + \mathbf{s}P(\psi(\mathbf{x})) - \psi(\mathbf{x})) \cdot \mathbf{s} &\neq (\psi(\mathbf{y}) + \mathbf{s}P(\psi(\mathbf{y})) - \psi(\mathbf{x})) \cdot \mathbf{s} \\
P(\psi(\mathbf{x})) &\neq (\psi(\mathbf{y}) - \psi(\mathbf{x})) \cdot \mathbf{s} + P(\psi(\mathbf{y})) \\
P(\psi(\mathbf{x})) &\neq (\psi(\mathbf{x}) + t\mathbf{s} - \psi(\mathbf{x})) \cdot \mathbf{s} + P(\psi(\mathbf{x}) + t\mathbf{s}) \\
P(\psi(\mathbf{x})) &\neq t + P(\psi(\mathbf{x}) + t\mathbf{s}) \\
\frac{P(\psi(\mathbf{x}) + t\mathbf{s}) - P(\psi(\mathbf{x}))}{t} &\neq -1
\end{aligned} \tag{6}$$

Taking the limit as t approaches 0

$$\nabla P(\psi(\mathbf{x})) \cdot \mathbf{s} \neq -1 \tag{7}$$

Hence, the deformed grid is valid if and only if $\nabla P(\psi(\mathbf{x})) \cdot \mathbf{s} \neq -1$. □

By using a continuity argument along with no deformation at the outer boundary, the restriction for valid grid movement can be changed so that

$$\nabla P(\psi(\mathbf{x})) \cdot \mathbf{s} > -1 \tag{8}$$

One result of this theorem is that interpretation of the deformation is important in determining whether the grid movement has failed. If the deformation direction is perpendicular to the gradient of the deformation function, then an infinite amount of deformation is allowable, with the typical restriction of working with finite precision machines on discrete data points.

4. THE 2D LAPLACIAN

The 2D Laplacian in polar coordinates can be written as

$$\frac{1}{r}\frac{\partial}{\partial r}\left(r\frac{\partial d}{\partial r}\right) + \frac{1}{r^2}\frac{\partial^2 d}{\partial \theta^2} = 0 \tag{9}$$

Definitions
The following terms are used for the various components of the solution to the Laplacian and the modified Laplacian:

1. The purely radial solution is denoted $g(r)$, and for the grid movement application presented herein, it must satisfy the boundary conditions: $g(1) = 1$ and $g(R) = 0$.
2. The frequency solutions are denoted $F_n(r, \theta)$, where the frequency n is any positive integer.
3. The radial components of the frequency solutions are denoted $R_n(r)$ and must satisfy the boundary conditions: $R_n(1) = 1$ and $R_n(R) = 0$.
4. The angular components of the frequency solutions are denoted $T_n(\theta)$. The frequency solution for each value of n is the product of the radial component and the angular component.
5. The radial solution for a particular surface deformation is defined as $d_0(r)$ and the frequency solutions for a particular surface deformation are defined as $d_n(r, \theta)$.
6. The validity function $v_n(r, \theta)$ is the scalar function associated with the grid movement restriction, and equals the gradient of the deformation dotted into the deformation direction. This function must be greater than -1 for all values of r and θ.

The general solution of the 2D Laplacian in polar coordinates between two concentric circles with inner radius of 1 and outer radius of R, with boundary conditions $d(1, \theta) = f(\theta)$ and

$d(R,\theta)=0$ is

$$d(r\theta)=d_o(r)+\sum_{n=1}^{\infty} d_n(r,\theta)$$
$$=a_0\left(1-\frac{\log r}{\log R}\right)+\sum_{n=1}^{\infty}(a_n\cos(n\theta)+b_n\sin(n\theta))\left(\frac{R^{2n}-r^{2n}}{r^n(R^{2n}-1)}\right) \tag{10}$$

where the coefficients are determined from the boundary function $f(\theta)$ and can be given as

$$a_0=\frac{1}{2\pi}\int_0^{2\pi} f(\theta)\,\mathrm{d}\theta$$
$$a_n=\frac{1}{\pi}\int_0^{2\pi} f(\theta)\cos(n\theta)\,\mathrm{d}\theta \tag{11}$$
$$b_n=\frac{1}{\pi}\int_0^{2\pi} f(\theta)\sin(n\theta)\,\mathrm{d}\theta$$

4.1. Application of 2D Laplacian to grid movement

There are several different types of surface deformation, including translation, expansion and rotation. If the deformation direction is in the angular direction only, then this is interpreted as a rotation of the inner circle. If the deformation direction is in the radial direction, then it can be interpreted as an expansion or contraction of the inner circle. Translation of the inner circle is caused by a deformation direction that varies in the radial and angular component. For instance, translation in the x-direction is caused by a deformation direction of the form $(\cos\theta,\sin\theta)$.

One unique result when applying the Laplacian to polar coordinates is that the radial deformation on the inner circle must be greater than -1, since the radius of the inner circle is 1. Otherwise, the radial component will be less than or equal to zero, which is not allowed. This restriction must be considered when studying the frequency deformations.

4.1.1. Purely radial solution. The use of the Laplacian to propagate a constant deformation on the surface of the inner circle will be analysed first. The purely radial solution is

$$d_0(r)=a_0\left(1-\frac{\log r}{\log R}\right) \tag{12}$$

where a_0 is the amount of deformation.

Theorem 4.1.1

For the radial solution for the 2D Laplacian, if the deformation direction is in the radial direction, then the maximum allowable deformation is $\log R$, and if the deformation direction is in the angular direction only, then any amount of deformation is allowed.

Proof
The proof of this theorem and all remaining theorems are in the Appendix.

4.1.2. Frequency deformation. The behaviour of the frequency deformations is important to understand when the inner circle is deforming due to forces acting on the circle or for shape-based design optimization. If the inner circle is only being translated, rotated or expanded in a uniform direction, then those deformations are in the radial direction only, and the frequency solutions are not active.

The frequency solution to the Laplacian is

$$d_n(r,\theta) = (a_n \cos(n\theta) + b_n \sin(n\theta)) \left(\frac{R^{2n} - r^{2n}}{r^n (R^{2n} - 1)} \right) \tag{13}$$

Theorem 4.1.2
For the frequency solution of the 2D Laplacian, the maximum allowable deformations for the purely radial and the purely angular deformations are given below

$$\begin{aligned} &(a_1 \cos(n\theta) + b_1 \sin(n\theta)) < \frac{R^{2n} - 1}{n(R^{2n} + 1)} \quad \text{if the deformation is purely radial} \\ &(a_1 \sin(n\theta) - b_1 \cos(n\theta)) < \frac{1}{n} \quad \text{if the deformation is purely angular} \end{aligned} \tag{14}$$

From this theorem, the maximum allowable deformation is $(R^2-1)/(R^2+1) < 1$ for the lowest frequency and decreases approximately as $1/n$ as the frequencies increase, for both the radial and angular deformations. Thus, if there is a frequency component within the grid movement, then the deformations are greatly limited, especially if there is high frequency content within the motion.

5. THE 2D MODIFIED LAPLACIAN

The Laplacian is modified to include a term that controls the rate of deformation in the radial direction, and has the form

$$\frac{1}{r} \frac{\partial}{\partial r} \left(r^{q+1} \frac{\partial d}{\partial r} \right) + r^{q-2} \frac{\partial^2 d}{\partial \theta^2} = 0 \tag{15}$$

If $q = 0$, then the traditional Laplacian is recovered. The general solution to the 2D modified Laplacian with $q \neq 0$ in polar coordinates between two concentric circles with inner radius of 1 and outer radius of R, with boundary conditions $d(1,\theta) = f(\theta)$ and $d(R,\theta) = 0$ is

$$\begin{aligned} d(r,\theta) &= d_0(r) + \sum_{n=1}^{\infty} d_n(r,\theta) \\ &= a_0 \frac{R^q - r^q}{r^q (R^q - 1)} + \sum_{n=1}^{\infty} (a_n \cos(n\theta) + b_n \sin(n\theta)) \left(\frac{R^{\alpha_1} r^{\varepsilon_1} - r^{\varepsilon_2}}{R^{\alpha_1} - 1} \right) \end{aligned} \tag{16}$$

where $\varepsilon_1 = -q - \alpha_1/2$, $\varepsilon_2 = -q + \alpha_1/2$ and $\alpha_1 = \sqrt{q^2 + 4n^2}$. The following inequalities hold for ε_1 and ε_2:

$$\begin{aligned} \varepsilon_1 &< 0 \quad \text{for all } q \text{ and for all integers } n > 0 \\ \varepsilon_2 &> 1 \quad \text{whenever } n^2 > q + 1 \\ 0 < \varepsilon_2 &\leqslant 1 \quad \text{whenever } n^2 \leqslant q + 1 \end{aligned} \tag{17}$$

5.1. *Application of 2D modified Laplacian to grid movement*

The introduction of the additional term within the modified Laplacian acts to stiffen the Laplacian. When the term is less than 1, it stiffens the equations so that the deformation extends further into the domain. When the term is greater than 1, it relaxes the equations so that the deformation is damped out more quickly. In relative terms, since this term varies throughout the domain, it implies that regions with smaller values are stiffer than those with larger values. As will be shown, this increased stiffness near the inner circle is beneficial.

Furthermore, if the exponent q is sufficiently negative, then the equations become so stiff that the deformations cause invalid meshes at the outer boundary which is not moving. Hence, there is an optimal value for the exponent q, based on the type of deformation. For the purely radial solution, this optimal value allows for perfect deformation of the inner circle. For the frequency solutions, the optimal value is a function of the frequency and the outer radius R, so that it is probably not practical to attempt to calculate this optimal value.

5.1.1. Purely radial solution. The purely radial solution for the 2D modified Laplacian is

$$d_0(r) = a_0 \frac{R^q - r^q}{r^q(R^q - 1)} \tag{18}$$

where a_0 is the amount of deformation. If $q = 0$, then this analysis reverts back to the traditional Laplacian, which involves logarithms.

Theorem 5.1.1

For the 2D modified Laplacian, any amount of deformation is allowed for the radial solution when the deformation direction is in the angular direction. If the deformation direction is in the radial direction, then the maximum allowable deformation for the radial solution falls into one of the following cases:

$$a_0 < \begin{cases} \dfrac{R}{|q|}\dfrac{R^{|q|} - 1}{R^{|q|}} & \text{if } q < -1 \\ R - 1 & \text{if } q = -1 \\ \dfrac{R^{|q|} - 1}{|q|} & \text{if } -1 < q < 0 \\ \log R & \text{if } q = 0 \\ \dfrac{R^q - 1}{qR^q} & \text{if } q > 0 \end{cases} \tag{19}$$

When $q = -1$, the maximum allowable deformation is $R-1$, which is the distance from the inner circle to the outer circle. For this value of q, with deformation in the radial direction only, the inner circle can be completely increased to the size of the outer circle, without any grid failure.

As an aside, the maximum allowable deformation as q approaches -1 from either side is $R-1$, so that there is no discontinuity. Similarly, as q approaches 0 from either side, then maximum allowable deformation approaches $\log R$, which is the solution for $q=0$.

An unexpected result of the modified Laplacian is that when $q < -1$, the equation is so stiff that the grid movement failure occurs first at the outer circle.

5.2. Frequency solutions

Theorem 5.2.1

For the 2D modified Laplacian with $q \geqslant -1$, when the deformation direction is purely radial, the maximum allowable deformation for the frequency solutions occurs at $r=1$. Under these circumstances, then the maximum allowable deformation is the following:

$$(a_n \cos(n\theta) + b_n \sin(n\theta)) < \frac{2(R^{\alpha_1}-1)}{\alpha_1(R^{\alpha_1}+1)+q(R^{\alpha_1}-1)} \tag{20}$$

The maximum allowable deformation is a function of three parameters R, q and n. Once the domain is chosen, the outer radius R is fixed. For fixed q, the maximum allowable deformation trends as $1/n$ for large values of n, which will occur for general grid movement applications when the surface is deformed rather than translated, rotated or expanded. For fixed n, an optimal value of q can be determined, which allows for the greatest deformation. However, this optimal value of q increases with n, so that an optimal value for one frequency will not be optimal for other values of n. If the deformation is dominated by a particular frequency, then using the optimal value based on that frequency may be beneficial. But if more than one frequency has strong influence, then the optimal value of q for that deformation may not be significantly better than a standard value, such as that used by Crumpton and Giles, which was $q=-2$ in 2D and $q=-3$ in 3D.

Theorem 5.2.2

For the 2D modified Laplacian with $q < -1$, when the deformation direction is purely radial, the maximum allowable deformation for the frequency solutions occurs at $r=1$, if the outer radius R satisfies $R^{\alpha_1}\varepsilon_1 + \alpha_1 R^{\varepsilon_2 - 1} < \varepsilon_2$, where $\varepsilon_2 = -q + \alpha_1/2$ and $\alpha_1 = \sqrt{q^2+4n^2}$. Under these circumstances, then the maximum allowable deformation is as follows:

$$(a_n \cos(n\theta) + b_n \sin(n\theta)) < \frac{2(R^{\alpha_1}-1)}{\alpha_1(R^{\alpha_1}+1)+q(R^{\alpha_1}-1)} \tag{21}$$

The restriction in this theorem determining the relationship between R, q and n does not influence the maximum allowable deformation for practical applications, in general. First, the maximum allowable deformation for the frequency solutions has an imposed restriction of the inner radius, since the simulation is in polar coordinates. If the maximum allowable deformation were greater than 1, then the inner circle would pass through the original, creating an invalid mesh, due to the singularity and not due to the general grid movement theorem.

Table I. Value of q for which the outer boundary acts as the restriction.

n	q
1	−2.52
2	−6.28
3	−11.18

To demonstrate the influence of this restriction, the value of q for which the outer boundary begins to act as the restriction is determined, using $R=5$ and for the first three frequencies. Table I shows the results. These values were derived from the above restriction and have been verified numerically. As the frequency increases, the value of q increases more rapidly. As is shown in Figure 12, the polar coordinates restriction is active for the initial range of q for each frequency, forcing the influence of the restriction at the outer boundary to begin to dominate at much larger values of q. Since the optimal value for translations is $q=-1$, it is unlikely that significantly larger values of q would be used for practical applications.

The next theorem applies when the deformation direction is the angular direction.

Theorem 5.2.3
For the 2D modified Laplacian, when the deformation direction is purely angular, the maximum allowable deformation for the frequency solutions occurs at $r=1$. Under these circumstances, then the maximum allowable deformation is as follows:

$$(a_n \cos(n\theta) - b_n \sin(n\theta)) < \frac{1}{n} \tag{22}$$

6. THREE-DIMENSIONAL MODIFIED LAPLACIAN

Following the same type of derivation, the Laplacian in spherical coordinates using modified to include a term that varies with the distance from the origin can be written as

$$\nabla \cdot (r^q \nabla d) = \frac{1}{r^2}\frac{\partial}{\partial r}\left(r^{q+2}\frac{\partial d}{\partial r}\right) + \frac{r^{q-2}}{\sin\theta}\frac{\partial}{\partial\theta}\left(\sin\theta\frac{\partial d}{\partial\theta}\right) + \frac{r^{q-2}}{\sin^2\theta}\frac{\partial^2 d}{\partial\phi^2} = 0 \tag{23}$$

If $q=0$, then the traditional Laplacian is recovered. The solution to the modified Laplacian in spherical coordinates between two concentric spheres with radii $r_{\text{inner}}=1$ and $r_{\text{outer}}=R$, with boundary conditions $d(1,\theta,\phi)=f(\theta,\phi)$ and $d(R,\theta,\phi)=0$ is

$$d(r,\theta,\phi) = a_0 g(r) + \sum_{n=1}^{\infty}\sum_{m=-n}^{m=n} a_{mn}\left(\frac{R^{\alpha_2} r^{\varepsilon_3} - r^{\varepsilon_4}}{R^{\alpha_2}-1}\right) T_n^m(\cos\theta)\mathrm{e}^{\mathrm{i}m\phi} \tag{24}$$

where the purely radial solution is

$$g(r) = \begin{cases} \dfrac{R^{q+1}-r^{q+1}}{r^{q+1}(R^{q+1}-1)} & \text{if } q \neq -1 \\ \dfrac{\log(R)-\log(r)}{\log(R)} & \text{if } q = -1 \end{cases} \tag{25}$$

and $\alpha_2 = \sqrt{4n^2 + q^2 + 4n + 2q + 1}$, $\varepsilon_3 = -q - 1 - \alpha_2/2$, $\varepsilon_4 = -q - 1 + \alpha_2/2$ and $T_n^m(\varphi)$ is the associated Legendre polynomial. The following inequality hold for ε_3 and ε_4:

$$\begin{aligned} \varepsilon_3 &< 0 \quad \text{for all } q \text{ and for all integers } n > 0 \\ \varepsilon_4 &> 1 \quad \text{whenever } n^2 + n > q + 2 \\ 0 < \varepsilon_4 &\leqslant 1 \quad \text{whenever } n^2 + n \leqslant q + 2 \end{aligned} \tag{26}$$

6.1. Application of 3D modified Laplacian to grid movement

6.1.1. Purely radial solution

Theorem 6.1.1
For the 3D modified Laplacian, any deformation is allowed for the radial solution if the deformation direction is in the angular direction. If the deformation is in the radial direction, then the maximum allowable deformation for the radial solution is

$$a_0 < \begin{cases} \dfrac{R^{q+1} - 1}{(q+1)R^{q+1}} & \text{if } q > -1 \\ \log(R) & \text{if } q = -1 \\ \dfrac{R^{|q|-1} - 1}{(|q| - 1)} & \text{if } -2 < q < -1 \\ R - 1 & \text{if } q = -2 \\ \dfrac{R^{|q|-1} - 1}{(|q| - 1)R^{|q|-2}} & \text{if } q < -2 \end{cases} \tag{27}$$

As for the 2D modified Laplacian, there is an optimal value for q, which allows for a complete enlargement of the inner sphere to the outer sphere. For the 3D modified Laplacian, the optimal value of q for purely radial motion is -2. Also, the maximum allowable deformation as q approach -1 from either side is $\log R$.

6.1.2. Frequency components. The maximum allowable deformations for the frequency components of the 3D modified Laplacian follow the same trends for the 2D modified Laplacian. The proofs are in the appendix.

Theorem 6.1.2a
For the 3D modified Laplacian with $q \geqslant -2$, when the deformation direction is purely radial, the maximum allowable deformation for the frequency solutions occurs at $r = 1$. Under these circumstances, then the maximum allowable deformation is as follows:

$$|a_{mn}||T_n^m(\cos\theta)| < \frac{2(R^{\alpha_2} - 1)}{\alpha_2(R^{\alpha_2} + 1) + (q+1)(R^{\alpha_2} - 1)} \tag{28}$$

where $\alpha_2 = \sqrt{4n^2 + q^2 + 4n + 2q + 1}$.

Theorem 6.1.2b

For the 3D modified Laplacian with $q < -2$, when the deformation direction is purely radial, the maximum allowable deformation for the frequency solutions occurs at $r = 1$, if the outer radius R satisfies $R^{\alpha_2}\varepsilon_3 + \alpha_2 R^{\varepsilon_4 - 1} < \varepsilon_4$, where $\varepsilon_3 = -q - 1 - \alpha_2/2$ and $\varepsilon_4 = -q - 1 + \alpha_2/2$. Under these circumstances, then the maximum allowable deformation is as follows:

$$|a_{mn}||T_n^m(\cos\theta)| < \frac{2(R^{\alpha_2} - 1)}{\alpha_2(R^{\alpha_2} + 1) + (q+1)(R^{\alpha_2} - 1)} \tag{29}$$

These results show that the maximum allowable deformation for the frequency components for the 3D modified Laplacian behaves similar to the maximum allowable deformation for the frequency components 2D modified Laplacian, varying inversely with the frequency n. For large R, this restriction trends as $2/(\alpha_2 + q + 1)$, so for fixed q, the maximum allowable deformation trends as $1/n$, which is the same result for the 2D modified Laplacian. (The behaviour of the maximum value of the associated Legendre polynomials is difficult to analyse and to bound. The calculation of the coefficients a_{mn} involves the reciprocal of $T_n^m(\cos\theta)$, so that $a_{mn}T_n^m(\cos\theta)$ is the appropriate quantity to bound.)

7. COMPUTATIONAL VALIDATIONS

The analytically determined maximum allowable deformations were tested on an unstructured triangulated grid where the outer radius was 5 for a variety of values of q between -10 and 0 and for frequencies up to $n = 20$. The deformed grids had no negative triangles, when the magnitude of the deformations were smaller than the maximum allowable deformation.

7.1. Single frequency deformations

Shown in Figures 2–6 are the grids for the maximum allowable deformations for $q = 0$ and at optimal values of q for purely radial expansion, for the first three frequencies and for $n = 9$.

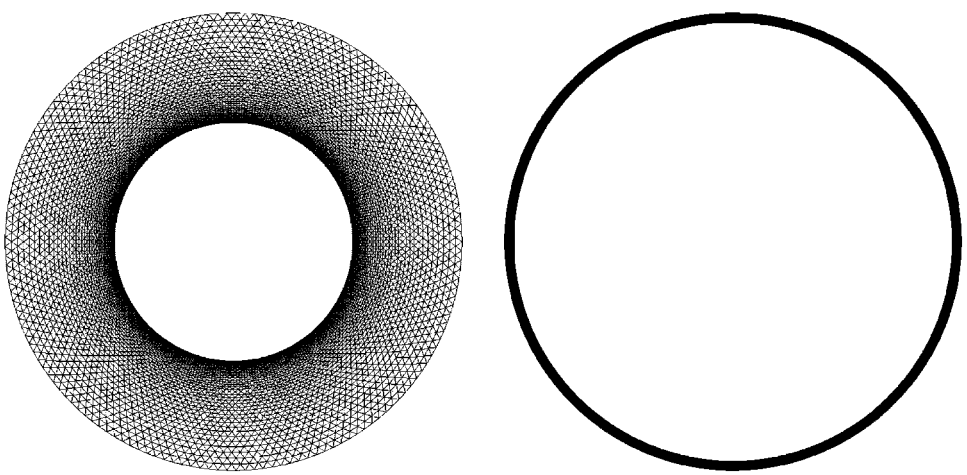

Figure 2. Radial deformation for $q = 0$ and -1.

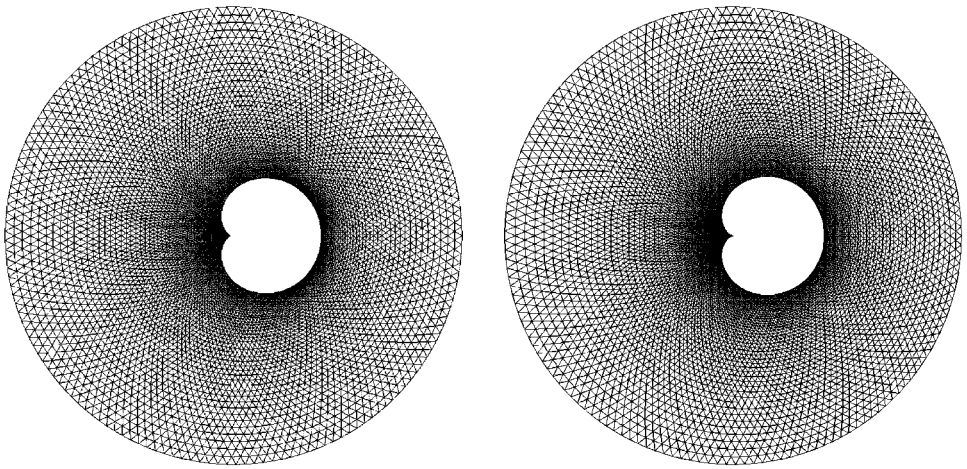

Figure 3. Frequency $n=1$ deformation for $q=0$ and -2.

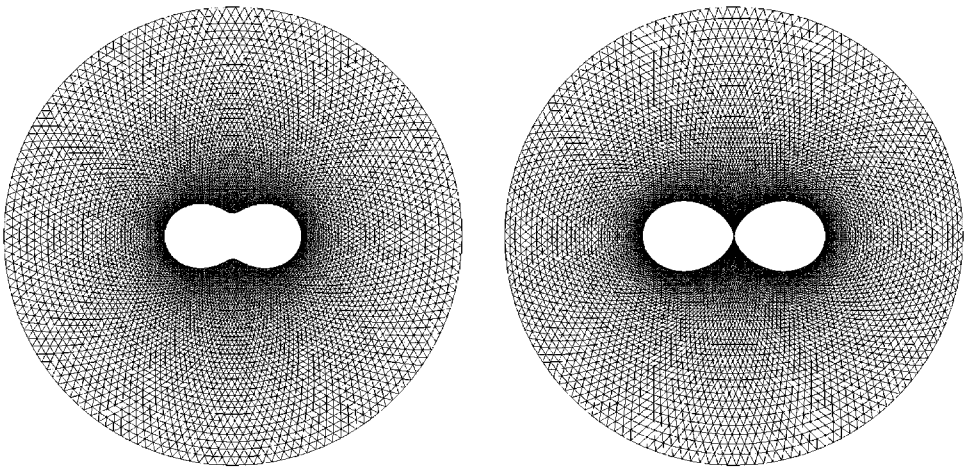

Figure 4. Frequency $n=2$ deformation for $q=0$ and -5.

When $q=-1$, the maximum allowable deformation is $R-1$, so that the inner circle can be completely expanded to the outer circle. In order to visualize this case, the deformation was only 95% of the maximum allowable deformation. For the frequency solution deformations, optimal values of q were used for the modified Laplacian, so that the maximum allowable deformation was 1 for these cases. For the case $n=9$, the optimal value of q was more negative than -40, but round-off error in the calculations prevented a full deformation of 1 for $n=9$. The use of the modified Laplacian for the frequency solutions significantly increases the maximum allowable deformation over the Laplacian. However, for grid movement

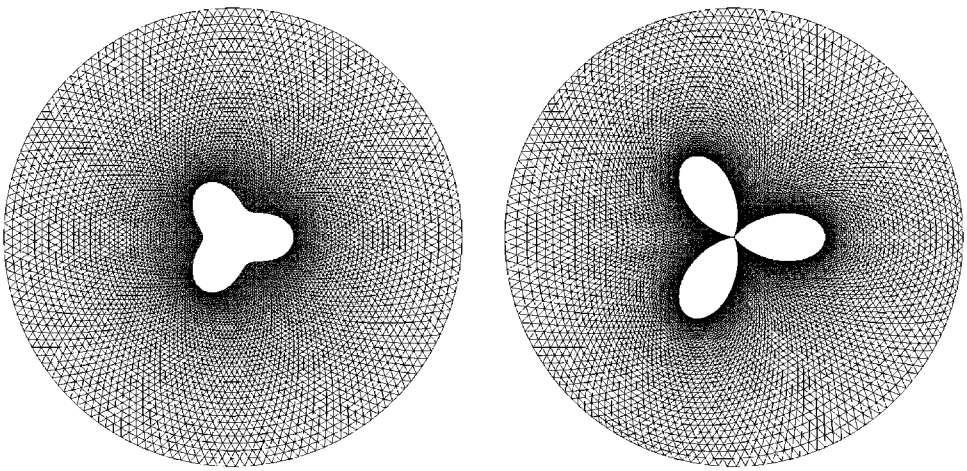

Figure 5. Frequency $n=3$ deformation for $q=0$ and -9.

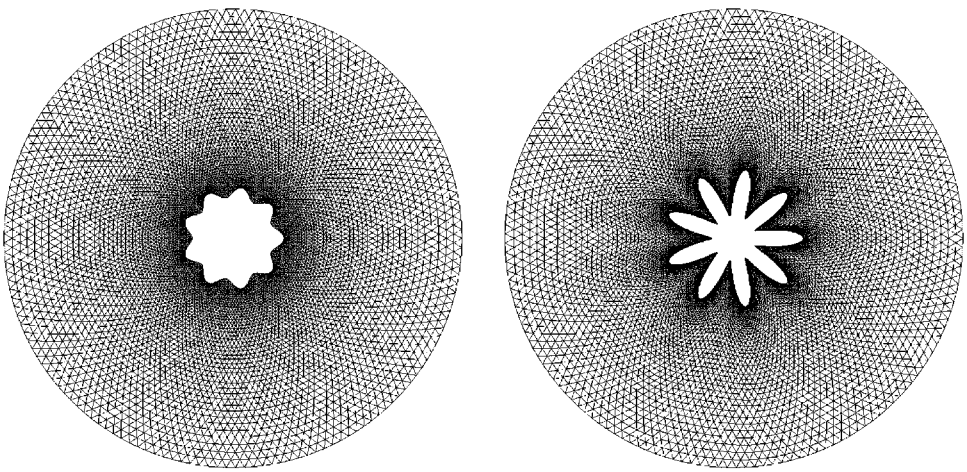

Figure 6. Frequency $n=9$ deformation for $q=0$ and -40.

problems with a wide range of frequencies, choosing the optimal value may be quite difficult and may not allow for deformation that are significantly better than the Laplacian.

The difference in the two deformations in Figure 3 is slight, because the maximum allowable deformation for the Laplacian is almost the same as for the modified Laplacian, due to the polar coordinates restriction that the maximum allowable deformation be less than or equal to the inner radius.

Figure 7 shows the compression of the grid for the radial solution at 95% of the maximum allowable deformation. This grid is highly compressed, but it is still a valid grid. In Figures 8

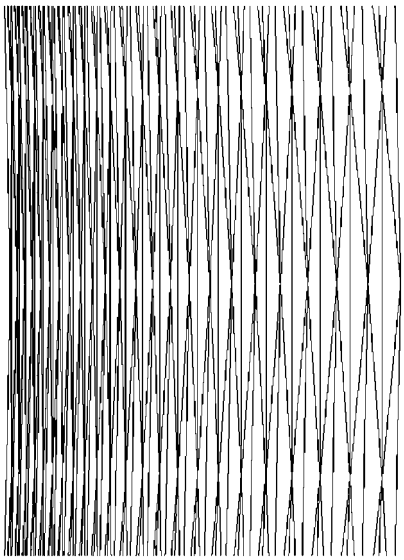

Figure 7. Close-up of radial deformation for $q = -1$.

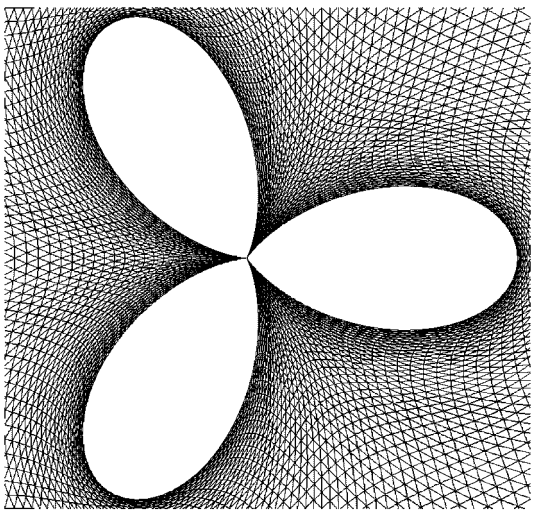

Figure 8. Close-up of frequency $n = 3$ deformation for $q = -9$.

and 9, closeup grids for two frequency solutions are shown. Because of appropriate choices of q, extreme distortions are allowed. The grid in Figure 9 for frequency $n = 9$ actually is an invalid mesh, even though theoretically it should be valid. Due to the coarseness of the mesh, the triangles near the greatest expansions are inverted because they are larger than the

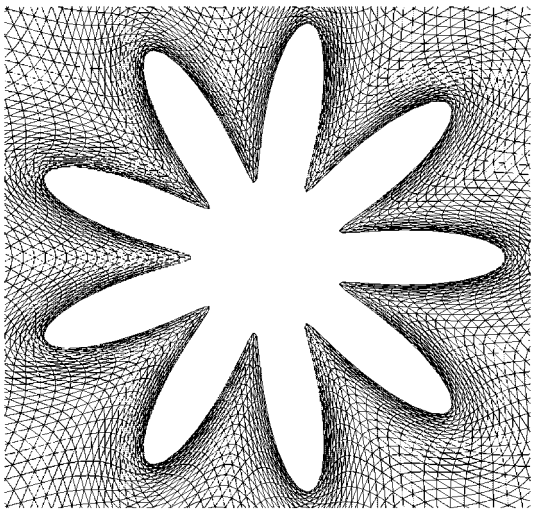

Figure 9. Close-up of frequency $n = 10$ deformation for $q = -40$.

fine scale details in the deformation. If a more refined grid were used, the modified Laplacian would produce a valid deformed grid.

7.2. Rotations and translations

In the previous section, only expansions and radial deformations of the inner circle are shown. To demonstrate that extreme rotations and translations can be achieved using the modified Laplacian, two more examples are presented. In the first, a translation in the x-direction of a distance of 3 is shown in Figure 10, using $q = -1$. As with the purely radial deformation case with $q = -1$, the translation can be quite severe, even translating the inner circle up against the outer circle without generating an invalid mesh.

For the rotation, the same value of q is used for a rotation of 180°. The resulting grid and closeup are shown in Figure 11. The rotation is limited by the discrete nature of the grid, so that if the grid were highly refined, much more rotation would be allowed.

7.3. Optimal choice of q for single frequency deformations

In Figure 12, the maximum allowable deformations for the case when $R = 5$ are shown as a function of q for the radial solution and the first four frequency solutions. For the radial solution, the optimal value of q is at -1, but for the frequency solutions, the maximum allowable deformation increases as q becomes more negative, until it reaches the maximum value of 1, which is the radius of the inner circle. As q decreases further, the maximum allowable deformation becomes restricted by the condition at the outer boundary and decreases.

Crumpton and Giles used a modified Laplacian $\nabla \cdot (k \nabla d) = 0$, where k was inversely proportional to the size of the elements. For a perfect triangular grid, as shown in Figure 13, with N points on the inner and on the outer circles, with inner radius of 1 and outer radius of R, then the area of a triangle attached to the inner circle would be approximately $2\pi^2/N^2$

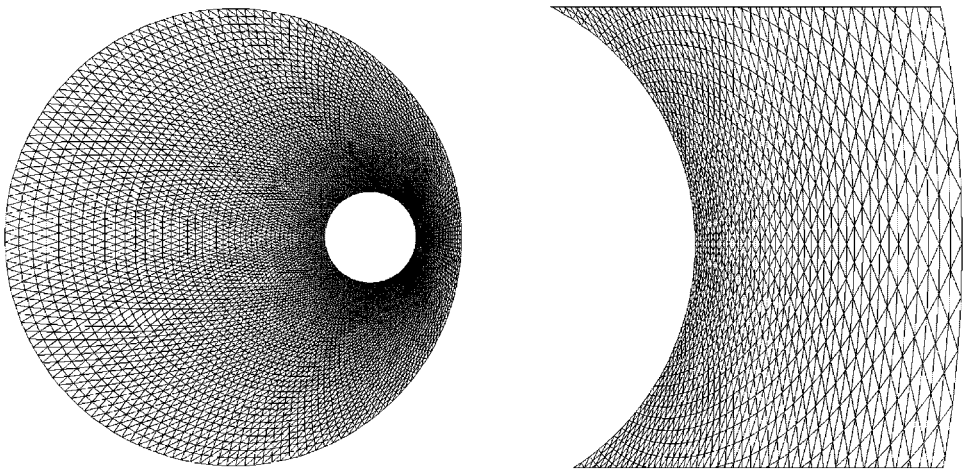

Figure 10. Images of translation of inner circle by 3.

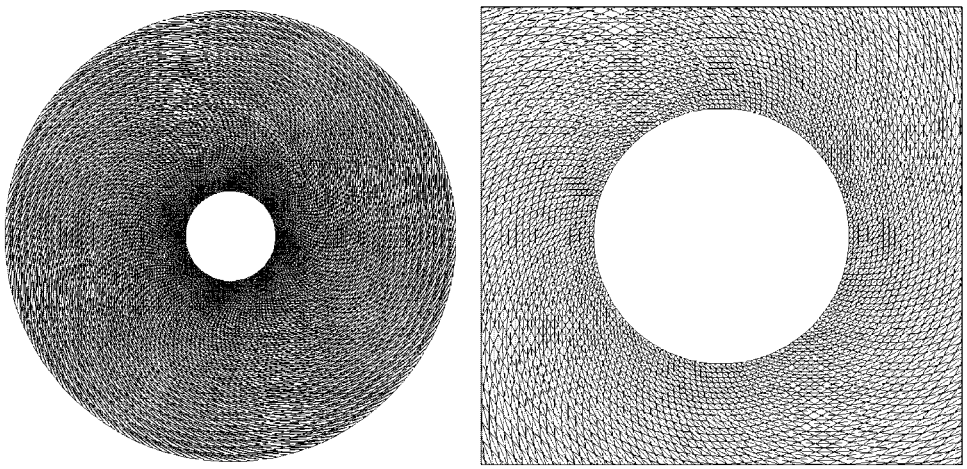

Figure 11. Images of rotation of inner circle by 180°.

while the area of a triangle at the outer circle would be approximately $2\pi^2R^2/N^2$. Hence, the area of the elements grows at a rate of r^2, and k would be r^{-2}. Similarly, in 3D, the value of k would vary at a rate of r^{-3}. Thus, Crumpton and Giles method was equivalent to a value of $q = -2$ for 2D and a value of $q = -3$ for 3D, both of which are reasonable compromises for practical applications with a wide range of frequency components in the deformation.

7.4. Practical applications

For realistic grid deformation applications, either the object will be translated or rotated without any deformation of the object or the object will be deformed. For the case of objects

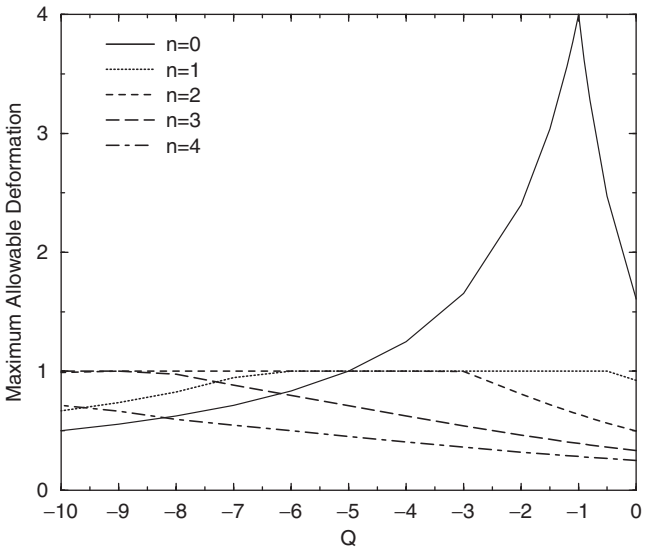

Figure 12. Variation of maximum allowable deformation with q and n.

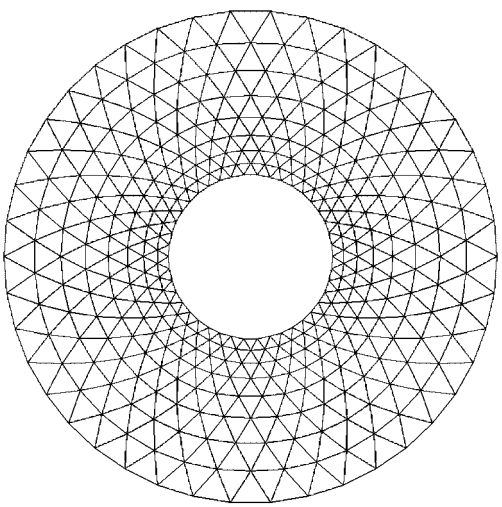

Figure 13. Example of concentric circles with perfect grid.

moving relative to one another, the grid motion has no frequency content, so the optimal value of q is -1 for 2D and -2 for 3D simulations, and the modified Laplacian should yield excellent results for this application. However, if the shape of the surface is deformed due to forces acting upon it, such as for aero-elastic wing deformation or free surface simulations, then the grid motion will have multiple frequency components. Hence, choosing an optimal value of q will not be practical, since the optimal value for each frequency component grows linearly with the frequency. As reported in the literature, the commonly chosen values

of $q=-2$ for 2D and $q=-3$ for 3D are a good choice, since the lowest frequencies will probably dominate most grid motions.

In general, practical applications will not involve circles and spheres, but rather complicated airfoils and B-Spline and NURBS curves and surfaces. Hence, the value of r used in the modified Laplacian must be interpreted for application to these types of geometries. In the literature, the two common practices for setting the value of stiffness, which is represented by the term r^q in our modified Laplacian, is to allow the stiffness to vary inversely with the distance from the surfaces in motion and to set the stiffness based on the local element size. Assuming that the element size is smallest near the surfaces in motion and grows as the distance from the surfaces increases, then the value of r should be interpreted as the distance to the nearest surface in motion, plus some representative size of the moving surface, such as the object's average radius. This interpretation is consistent with the analytical results presented herein, as well as in the literature.

8. COMPARISON WITH LINEAR SPRINGS

The linear springs method is quite similar to the modified Laplacian. For the simplest linear spring methodology, the deformations are propagated throughout the domain by assuming that each edge consists of a spring whose stiffness is inversely related to the length of the edge. This spring network is acted upon by an external force, which is the deformation at one or more boundaries. By seeking an equilibrium or a balance of the forces, the deformations can be found by solving repeatedly via

$$\begin{aligned} \Delta x_i^{m+1} &= \frac{\sum_j k_{ij}\Delta x_j^m}{\sum_j k_{ij}} \\ \Delta y_i^{m+1} &= \frac{\sum_j k_{ij}\Delta y_j^m}{\sum_j k_{ij}} \end{aligned} \tag{30}$$

where i is the node to be solved, j is a list of nodes attached to node i, k_{ij} is the stiffness of the edge between nodes i and j, and Δx_j^m is the deformation at node j at iteration m. Typically, k_{ij} varies inversely with the length of the edge ij. This spring network is not coupled and hence does not allow for changes in x to affect y and *vice versa*. The version of the spring analogy that allows coupling between the x and y directions cannot be directly related to the modified Laplacian.

The modified Laplacian can be solved numerically in the following manner:

$$0=\int_\Omega \nabla\cdot(r^q\nabla d)=\int_{\partial\Omega}(r^q\nabla d)\cdot\hat{n}\,\mathrm{d}S\approx\sum_j r_{ij}^q\frac{d_j-d_i}{s_{ij}}A_{ij} \tag{31}$$

where r_{ij} is the radial value at the middle of edge ij, s_{ij} is the distance between nodes i and j and A_{ij} is the length of the face of the dual associated with edge ij. Solving for d_i

$$d_i=\frac{\sum_j r_{ij}^q\frac{d_jA_{ij}}{s_{ij}}}{\sum_j r_{ij}^q\frac{A_{ij}}{s_{ij}}} \tag{32}$$

which is similar in structure to the equation for the linear spring analogy. If the grid is a perfect grid, as shown in Figure 13, then the length of each edge ij should be approximately $2\pi r_{ij}/N$. Similarly, the value of A_{ij} should scale with r_{ij}, so that the equation for d_i becomes

$$d_i \approx \frac{\sum_j r_{ij}^q d_j}{\sum_j r_{ij}^q} \tag{33}$$

Typically k_{ij} varies inversely with the length of edge ij raised to some exponent q. For a perfect grid, the length of the edge varies with the radius r_{ij}, so $k_{ij} = r_{ij}^q$. This derivation shows that the Laplacian and the linear springs analogy yield the same results for a perfect grid between two concentric circles. By analogy, it is assumed that the restrictions on the Laplacian are similar to the restrictions on the linear spring analogy for various exponents q. Blom [21] has come to similar conclusion when he compared the linear spring analogy to elliptic grid generation algorithms, and alters his spring stiffness coefficient near the moving surface by increasing the stiffness by a factor of 5, which is similar to a modified Laplacian approach.

9. ANALYSIS OF VARIANT OF LAPLACIAN

Masud and Hughes [3] present a variant to the two-dimensional Laplacian, where the Laplacian is modified by including a term that scales as $1+(1/r)$ rather than as $1/r$, so that the governing equation for the grid movement is

$$\nabla \cdot (1 + \tau_m)\nabla d = 0 \tag{34}$$

where

$$\tau_m^e = \frac{1 - \Delta_{\min}/\Delta_{\max}}{\Delta^e/\Delta_{\max}} \tag{35}$$

where $\Delta_{\min}$ is the area of the smallest element, $\Delta_{\max}$ is the area of the largest element in the grid, Δ^e is the area of the particular element. Assuming a grid about two concentric circles as described above, with inner radius of 1 and outer radius of R, and assuming that the area of each element scales with the square of radial distance, so that $\Delta = Ar^2$, then this grid movement equation reduces to

$$\nabla \cdot \left[\left(\frac{r^2 + R^2 - 1}{r^2} \right) \nabla d \right] = 0 \tag{36}$$

Transforming to polar coordinates, this equation becomes

$$\frac{1}{r} \frac{\partial}{\partial r} \left(\frac{r^2 + R^2 - 1}{r} \frac{\partial d}{\partial r} \right) + \frac{r^2 + R^2 - 1}{r^2} \frac{\partial^2 d}{\partial r^2} = 0 \tag{37}$$

The radial solution, assuming the same boundary conditions, is

$$d_o(r) = a_0 \frac{\ln(r^2 + R^2 - 1) - \ln(2R^2 - 1)}{\ln(R^2) - \ln(2R^2 - 1)} \tag{38}$$

The validity function is

$$v(r) = \frac{-a_0}{(\ln(2R^2 - 1) - \ln(R^2))} \frac{2r}{r^2 + R^2 - 1} > -1 \tag{39}$$

This is most restrictive at $r = R$, so the largest displacement for the radial solution is

$$a_0 < \frac{2R^2 - 1}{2R} \ln\left(\frac{2R^2 - 1}{R^2}\right) \tag{40}$$

This grid movement formulation differs from the modified Laplacian in that the validity function is limited by the behaviour at the outer radius rather than at the inner radius. How does it compare with the Laplacian and with the optimal choice for the modified Laplacian (i.e. $q = -1$) for the radial deformation case? For the Laplacian, the restriction is that $a_0 < \log(R)$, while the restriction for the optimal modified Laplacian is $a_0 < R - 1$. Crumpton and Giles methodology is approximately equivalent to a modified Laplacian with $q = -2$, which has a restriction of $a_0 = R^2 - 1/2R$. The maximum allowable deformation for these different approaches to the Laplacian is shown in Figure 14. The optimal choice ($q = -1$) allows the maximum deformation, while the original Laplacian ($q = 0$) is the most restrictive. Masud and Hughes's variant of the Laplacian yields better results than that of Crumpton and Giles, but it is not as good as the optimal choice. However, since the work performed by Masud and Hughes and by Crumpton and Giles included deformations in the

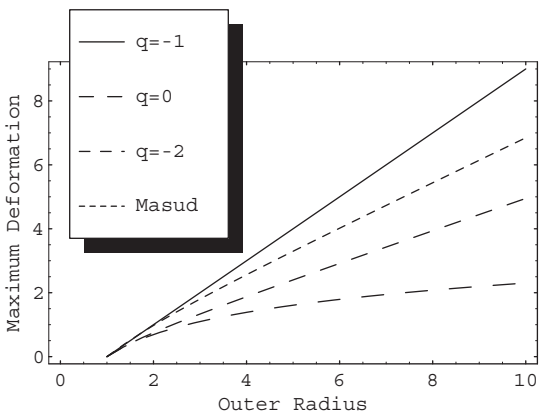

Figure 14. Maximum allowable deformation for the Laplacian ($q = 0$), the optimal Laplacian ($q = -1$), Crumpton and Giles choice ($q = -2$) and Masud and Hughes variation, for the radial deformation.

frequency components as well as in the radial components, their methods are both reasonable compromises over the space of frequencies in their problems.

10. CONCLUSIONS

Analytic solutions for the modified Laplacian in 2D and 3D for the case of concentric circles and spheres where the inner circle or sphere is deformed while the outer circle or sphere is undeformed has been derived. Using a general grid movement theorem that states when a grid will become invalid due to a grid deformation, the maximum allowable deformation on the inner circle or sphere has been determined using these analytic solutions.

For the case of radial deformation only, where the deformation is constant on the surface of the circle or sphere, then any amount of deformation is allowed if the deformation direction is in an angular direction. When the exponent q is -1 for 2D and -2 for 3D, then the inner circle or sphere can be expanded until it reaches the outer circle or sphere without creating an invalid grid. Hence, for rotations, translations and expansions of the inner circle, the modified Laplacian yields excellent results.

However, if the deformation on the circle or sphere is not constant, then the frequency variations must be considered. As the frequency of the deformation increases for fixed q and R, then the maximum allowable deformation decreases at approximately a rate of $1/n$, where n is the frequency. For single frequencies, an optimal value of q can be found which allows for severe deformation. For general grid movement simulations, where the frequency content is quite high, a compromise in the choice of q among the various optimal values is needed, which will greatly reduce the amount of deformation. Crumpton and Giles used the modified Laplacian with a stiffness coefficient that varied inversely with the size of the element. Their choice amounted to a value of $q = -2$ for 2D grids and $q = -3$ for 3D grids, which was a good compromise for their applications. A variant of the Laplacian used by Masud and Hughes was compared with the modified Laplacian. This variant did not perform as well as the optimal choice of the modified Laplacian since the optimal choice allowed for a complete deformation of the inner circle to the outer circle, but it performed better than the method used by Crumpton and Giles for the purely radial motion.

The conclusion to be drawn from this analytic investigation into a simplified grid deformation problem is that for rotations, translations and expansions of an isolated object far from the outer boundary, the modified Laplacian with appropriate choice of q should yield excellent results. But if the grid deformations have higher order frequency components, then the use of the modified Laplacian will restrict the amplitude of the deformations.

Finally, the modified Laplacian and the linear spring analogy are shown to be equivalent for a special case of two concentric circles. Hence, for general deformations, it can be assumed that the restrictions for the modified Laplacian apply to the linear spring analogy.

APPENDIX A

Theorem 4.1.1

For the radial solution for the 2D Laplacian, if the deformation direction is in the radial direction, then the maximum allowable deformation is $\log R$, and if the deformation direction is in the angular direction only, then any amount of deformation is allowed.

Proof
The gradient of the radial solution is

$$\nabla d_0(r) = \left(-\frac{a_0}{r \log R}, 0 \right) \tag{A1}$$

Clearly, if the deformation direction is only in the angular direction, then $\mathbf{s} = (0,1)$ and $\nabla d_0(r) \cdot \mathbf{s} = 0$. This product is always greater than -1, so any amount of deformation is allowed.

If the deformation direction is only in the radial direction, then $\mathbf{s} = (1,0)$, and the validity function $v_0(r)$ is

$$v_0(r) = -\frac{a_0}{r \log R} > -1 \tag{A2}$$

This function must be greater than -1, so $a_0 < r \log R$ for all $r \in [1, R]$. This relation is most restrictive when $r = 1$, so the maximum allowable deformation is $a_0 < \log R$. □

Theorem 4.1.2
For the frequency solutions of the 2D Laplacian, the maximum allowable deformations for the purely radial and the purely angular deformations are given below

$$\begin{aligned} &(a_1 \cos(n\theta) + b_1 \sin(n\theta)) < \frac{R^{2n} - 1}{n(R^{2n} + 1)} && \text{if the deformation is purely radial} \\ &a_1 \sin(n\theta) - b_1 \cos(n\theta)) < \frac{1}{n} && \text{if the deformation is purely angular} \end{aligned} \tag{A3}$$

Proof
The gradient of frequency solution is

$$\begin{aligned} \nabla d_n(r,\theta) = ((a_n \cos(n\theta) + b_n \sin(n\theta)) \left(-n \frac{R^{2n} + r^{2n}}{r^{n+1}(R^{2n} - 1)} \right), \\ n(-a_n \sin(n\theta) + b_n \cos(n\theta)) \left(\frac{R^{2n} - r^{2n}}{r^{n+1}(R^{2n} - 1)} \right) \end{aligned} \tag{A4}$$

If the deformation is a radial deformation (i.e. $\mathbf{s} = (1,0)$), then the validity function is

$$v_n(r,\theta) = (a_n \cos(n\theta) + b_n \sin(n\theta)) \left(-n \frac{R^{2n} + r^{2n}}{r^{n+1}(R^{2n} - 1)} \right) > -1 \tag{A5}$$

and the restriction for successful grid movement is

$$(a_n \cos(n\theta) + b_n \sin(n\theta)) < \frac{r^{n+1}(R^{2n} - 1)}{n(R^{2n} + r^{2n})} \tag{A6}$$

The right-hand side function is positive for all $r>0$, is equal to zero at $r=0$ and has one extremum, at $r=\sqrt[2n]{(n+1/n-1)}R>R$, which lies outside of the domain of interest. In the domain of interest, the right-hand side is an increasing function of r, so it is most restrictive at $r=1$. Thus, the restriction is

$$(a_n \cos(n\theta) + b_n \sin(n\theta)) < \frac{(R^{2n}-1)}{n(R^{2n}+1)} \tag{A7}$$

If the deformation is purely angular (i.e. $\mathbf{s}=(0,1)$), then the validity function is

$$v_n(r,\theta) = n(-a_n \sin(n\theta) + b_n \cos(n\theta)) \left(\frac{R^{2n}-r^{2n}}{r^{n+1}(R^{2n}-1)} \right) \tag{A8}$$

and the restriction is

$$(a_n \sin(n\theta) - b_n \cos(n\theta) < \frac{r^{n+1}(R^{2n}-1)}{n(R^{2n}-r^{2n})} \tag{A9}$$

The right-hand side is 0 at $r=0$ and is monotonically increasing until $r=R$ where it grows without bound. Hence, this is most restrictive on the interval $[1,R]$ when $r=1$, or

$$(a_n \sin(n\theta) - b_n \cos(n\theta)) < \frac{1}{n} \tag{A10}$$

□

Theorem 5.1.1

For the 2D modified Laplacian, any amount of deformation is allowed for the radial solution when the deformation direction is in the angular direction. If the deformation direction is in the radial direction, then the maximum allowable deformation for the radial solution falls into one of the following cases:

$$a_0 < \begin{cases} \dfrac{R}{|q|} \dfrac{R^{|q|}-1}{R^{|q|}} & \text{if } q < -1 \\ R-1 & \text{if } q = -1 \\ \dfrac{R^{|q|}-1}{|q|} & \text{if } -1 < q < 0 \\ \log R & \text{if } q = 0 \\ \dfrac{R^q-1}{qR^q} & \text{if } q > 0 \end{cases} \tag{A11}$$

Proof

The case when $q=0$ was proved in a previous section, so it will be assumed that $q \neq 0$ for the following derivations.

The gradient of the deformation is

$$\nabla d_0(r) = \left(-\frac{a_0 q R^q}{r^{q+1}(R^q-1)}, 0 \right) \tag{A12}$$

If the deformation direction is in the angular direction (i.e. $\mathbf{s}=(0,1)$), then the validity function is

$$v_0(r)=0 > -1 \tag{A13}$$

So, it will always satisfy the grid movement restriction.

If the deformation direction is in the radial direction (i.e. $\mathbf{s}=(1,0)$), then the validity function is

$$v_0(r)= -\frac{a_0 q R^q}{r^{q+1}(R^q-1)} > -1 \tag{A14}$$

The validity function is negative for all $r>0$ and for all q. If q is positive, then each term in the validity function is positive, with the product multiplied by a negative sign. If q is negative, then $R^q-1<0$, and the product again is negative. Hence, the restriction for successful grid movement is

$$a_0 < \frac{r^{q+1}(R^q-1)}{qR^q} \tag{A15}$$

If $q=-1$, then the restriction reduces to

$$a_0 < \frac{R^{-1}-1}{-R^{-1}}=R-1 \tag{A16}$$

When $q>-1$, then the restriction is an increasing function of r, and when $q<-1$, it is a decreasing function of r.

Hence, when $q>-1$, the restriction is most restrictive when $r=1$, or

$$a_0 < \frac{R^q-1}{qR^q} \tag{A17}$$

If $-1<q<0$, then this restriction can be written as

$$a_0 < \frac{R^{-|q|}-1}{-|q|R^{-|q|}}=\frac{R^{|q|}-1}{|q|} \tag{A18}$$

When $q<-1$, the restriction is most restrictive when $r=R$, since it is a decreasing function of r, or

$$a_0 < \frac{R}{|q|}\,\frac{R^{|q|}-1}{R^{|q|}} \tag{A19}$$

□

Theorem 5.2.1

For the 2D modified Laplacian with $q\geqslant -1$, when the deformation direction is purely radial, the maximum allowable deformation for the frequency solutions occurs at $r=1$. Under these circumstances, then the maximum allowable deformation is as follows:

$$(a_n\cos(n\theta)+b_n\sin(n\theta)) < \frac{2(R^{\alpha_1}-1)}{\alpha_1(R^{\alpha_1}+1)+q(R^{\alpha_1}-1)} \tag{A20}$$

where $\alpha_1=\sqrt{q^2+4n^2}$.

Proof
The gradient of the frequency solution is

$$\nabla d_n(r,\theta) = \left((a_n \cos(n\theta) + b_n \sin(n\theta))\left(\frac{R^{\alpha_1}\varepsilon_1 r^{\varepsilon_1 - 1} - \varepsilon_2 r^{\varepsilon_2 - 1}}{R^{\alpha_1} - 1}\right),\right.$$
$$\left. n(-a_n \sin(n\theta) + b_n \cos(n\theta))\left(\frac{R^{\alpha_1} r^{\varepsilon_1 - 1} - r^{\varepsilon_2 - 1}}{R^{\alpha_1} - 1}\right)\right) \tag{A21}$$

where $\varepsilon_1 = -q - \alpha_1/2$, $\varepsilon_2 = -q + \alpha_1/2$ and $\alpha_1 = \sqrt{q^2 + 4n^2}$. If the deformation direction is purely radial, then the validity function is

$$v_n(r,\theta) = (a_n \cos(n\theta) + b_n \sin(n\theta))\left(\frac{R^{\alpha_1}\varepsilon_1 r^{\varepsilon_1 - 1} - \varepsilon_2 r^{\varepsilon_2 - 1}}{R^{\alpha_1} - 1}\right) > -1 \tag{A22}$$

The radial part is

$$\mathrm{Rad}_n(r) = \frac{R^{\alpha_1}\varepsilon_1 r^{\varepsilon_1 - 1} - \varepsilon_2 r^{\varepsilon_2 - 1}}{R^{\alpha_1} - 1} \tag{A23}$$

Since $\varepsilon_1 < 0$ and $\varepsilon_2 > 0$ for all q and n, the radial part is negative for all positive values of r. As stated above, $\varepsilon_1 < 0$, so $\varepsilon_1 - 1 < 0$ for all q and n, so the behaviour of this first term in the numerator is the same for all values of q and n. However, since ε_2 can be greater or less than 1 based on the values of q and n, there are three cases: $n^2 > q + 1$, $n^2 = q + 1$ and $n^2 < q + 1$.

Case 1: $n^2 > q + 1$. In this case, $\varepsilon_2 - 1 > 0$, so the radial part is negative for all values of $r > 0$ and approaches negative infinity as r approaches 0 and as r approach infinity. Thus, function has at least one extrema in the interval $(0, \infty)$. The extrema of the radial part are found by setting the derivative to zero and solving for r, which yields

$$r = R\left(\frac{\varepsilon_1(\varepsilon_1 - 1)}{\varepsilon_2(\varepsilon_2 - 1)}\right)^{1/\alpha_1} \tag{A24}$$

which shows that there is only one extrema in the interval $(0, \infty)$, which is a maximum. Thus, the minimum of the radial part on the interval $[1, R]$ must occur at the endpoints. At the endpoints, the radial part is

$$\frac{\partial \mathrm{Rad}_n}{\partial r}(1) = \frac{R^{\alpha_1}\varepsilon_1 - \varepsilon_2}{R^{\alpha_1} - 1}$$
$$\frac{\partial \mathrm{Rad}_n}{\partial r}(R) = \frac{R^{\alpha_1}\varepsilon_1 R^{\varepsilon_1 - 1} - \varepsilon_2 R^{\varepsilon_2 - 1}}{R^{\alpha_1} - 1} = \frac{(\varepsilon_1 - \varepsilon_2)R^{\varepsilon_2 - 1}}{R^{\alpha_1} - 1}$$
$$= -\frac{\alpha_1 R^{\varepsilon_2 - 1}}{R^{\alpha_1} - 1} \tag{A25}$$

To demonstrate when the value at $r=1$ is more negative than the value at $r=R$, consider the following function of R, which is a measure of the difference of Rad_n at the inner and outer radii:

$$\mathscr{F}(R)=R^{\alpha_1}\varepsilon_1-\varepsilon_2+\alpha_1 R^{\varepsilon_2-1} \tag{A26}$$

If $\mathscr{F}<0$, then the value at $r=1$ is greater than the value at $r=R$. Clearly, $\mathscr{F}(1)=0$, and $\lim_{R\to\infty}\mathscr{F}(R)=-\infty$. If $\mathscr{F}$ has no critical points between 1 and ∞, then the functional is a negative, monotonically decreasing function for $R>1$. To identify the critical points, set the derivative of $\mathscr{F}(R)=0$, or

$$\mathscr{F}'(R)=\alpha_1 R^{\alpha_1-1}\varepsilon_1+(\varepsilon_2-1)\alpha_1 R^{\varepsilon_2-2}=0 \tag{A27}$$

Rearranging

$$R^{\alpha_1+1-\varepsilon_2}=\frac{1-\varepsilon_2}{\varepsilon_1} \tag{A28}$$

The critical points of $\mathscr{F}(R)$ will be greater than 1, only if

$$\frac{1-\varepsilon_2}{\varepsilon_1}>1 \tag{A29}$$

which will occur whenever $q<-1$. Hence, when $q>-1$, the critical point of $\mathscr{F}(R)$ is less than one, so that $\mathscr{F}(R)<0$ for all values of $R>1$, and the radial part is more negative at $r=1$ than at $r=R$. Thus, the maximum allowable deformation occurs at $r=1$ and must satisfy

$$(a_n\cos(n\theta)+b_n\sin(n\theta))<\frac{2(R^{\alpha_1}-1)}{\alpha_1(R^{\alpha_1}+1)+q(R^{\alpha_1}-1)} \tag{A30}$$

Case 2: $n^2=q+1$. In this case, $\varepsilon_2-1=0$, so the radial part $\mathrm{Rad}_n(r)$ simplifies to

$$\mathrm{Rad}_n(r)=-\frac{R^{q+2}(q+1)r^{-q-2}+1}{R^{q+2}-1} \tag{A31}$$

This function approaches $-\infty$ as r approaches 0 and approaches $-(1/R^{q+2}-1)$ as r approaches ∞. It is a negative function for all positive values of r and is monotonically increasing with r. Hence, on the interval $[1,R]$, it is most restrictive at $r=1$, and the same maximum allowable deformation applies.

Case 3: $n^2<q+1$. Following the derivation given above, since $n^2<q+1$, then $\varepsilon_2-1<0$. Under these circumstances, the radial part approaches negative infinity as r approaches 0 and approaches 0 as r approaches infinity. The critical points for the radial part satisfy the following equation:

$$r=R\left(\frac{\varepsilon_1(\varepsilon_1-1)}{\varepsilon_2(\varepsilon_2-1)}\right)^{1/\alpha_1} \tag{A32}$$

The fraction under the radical is negative, because $\varepsilon_1<0$ and $0<\varepsilon_2<1$. Hence, there is no critical point for $r>0$, the radial part is a negative monotonically increasing function of r, the most negative value occurs when $r=1$, and the same restriction for the maximum allowable deformation holds. □

Theorem 5.2.2
For the 2D modified Laplacian with $q < -1$, when the deformation direction is purely radial, the maximum allowable deformation for the frequency solutions occurs at $r = 1$, if the outer radius R satisfies $R^{\alpha_1}\varepsilon_1 + \alpha_1 R^{\varepsilon_2 - 1} < \varepsilon_2$, where $\varepsilon_2 = -q + \alpha_1/2$ and $\alpha_1 = \sqrt{q^2 + 4n^2}$. Under these circumstances, then the maximum allowable deformation is as follows:

$$(a_n \cos(n\theta) + b_n \sin(n\theta)) < \frac{2(R^{\alpha_1} - 1)}{\alpha_1(R^{\alpha_1} + 1) + q(R^{\alpha_1} - 1)} \tag{A33}$$

Proof
Following the derivation given above, if $q < -1$, then the functional $\mathscr{F}(R)$ is positive for all R between 1 and $R_{\max}$. It is then negative for all values $R > R_{\max}$. If R satisfies the conditions of the theorem, then $\mathscr{F}(R) < 0$, and the radial part is more negative at $r = R$ than at $r = 1$.

Thus, under the conditions of the theorem, the maximum allowable deformation occurs at $r = 1$ and satisfies

$$(a_n \cos(n\theta) + b_n \sin(n\theta)) < \frac{2(R^{\alpha_1} - 1)}{\alpha_1(R^{\alpha_1} + 1) + q(R^{\alpha_1} - 1)} \tag{A34}$$

□

Theorem 5.2.3
For the 2D modified Laplacian, when the deformation direction is purely angular, the maximum allowable deformation for the frequency solutions occurs at $r = 1$. Under these circumstances, then the maximum allowable deformation is as follows:

$$(a_n \cos(n\theta) - b_n \sin(n\theta)) < \frac{1}{n} \tag{A35}$$

Proof
When the deformation direction is purely angular, the validity function is

$$v_n(r, \theta) = n(-a_n \sin(n\theta) + b_n \cos(n\theta)) \left(\frac{R^{\alpha_1} r^{\varepsilon_1 - 1} - r^{\varepsilon_2 - 1}}{R^{\alpha_1} - 1} \right) \tag{A36}$$

where the radial part of the validity function is

$$\mathrm{Rad}_n(r) = \frac{R^{\alpha_1} r^{\varepsilon_1 - 1} - r^{\varepsilon_2 - 1}}{R^{\alpha_1} - 1} \tag{A37}$$

As stated in the lemma, $\varepsilon_1 - 1 \leqslant 0$ when $n^2 \leqslant q + 1$ and $\varepsilon_1 - 1 > 0$ when $n^2 > q + 1$. Two different behaviours occur based on the sign of $\varepsilon_2 - 1$. These will be studied in two different cases.

Case 1: When $n^2 > q + 1$, $\varepsilon_2 - 1 > 0$, so the radial part ranges from positive infinity at $r = 0$ to negative infinity as r approaches infinity. Since this function has no critical points, it is monotonically decreasing. Its values at the endpoints are

$$\begin{aligned} \mathrm{Rad}_n(1) &= 1 \\ \mathrm{Rad}_n(R) &= 0 \end{aligned} \tag{A38}$$

So, it is largest at $r=1$. Hence, the validity function is most negative at $r=1$, where it must satisfy the following relation for success grid movement:

$$v_n(r,\theta)=n(-a_n\ \sin(n\theta)+b_n\ \cos(n\theta))\ >\ -1 \tag{A39}$$

The maximum allowable deformation is

$$(a_n\ \sin(n\theta)-b_n\ \cos(n\theta))\ <\ \frac{1}{n} \tag{A40}$$

Case 2: When $n^2\leqslant q+1$, $\varepsilon_2-1\leqslant 0$, so the radial part approaches 0 as r approaches infinity. To consider the behaviour as r approaches 0, rewrite the radial part as

$$\mathrm{Rad}_n(r)=\frac{(R^{\alpha_1}-r^{\alpha_1})r^{\varepsilon_1-1}}{R^{\alpha_1}-1} \tag{A41}$$

From this expression, $\mathrm{Rad}_n(0)=+\infty$. As stated above for case 1, $\mathrm{Rad}_n(1)=1$ and $\mathrm{Rad}_n(R)=0$. Hence, there is at least one critical point in the radial part, which is a minimum at

$$r=R\left(\frac{\varepsilon_1-1}{\varepsilon_2-1}\right)^{1/\alpha_1} \tag{A42}$$

But since there is only one critical point, it must be a minimum due to the shape of the function. Thus, the radial part is monotonically decreasing in the interval $[1,R]$, so the validity function is most negative at $r=1$, and the maximum allowable deformation is

$$(a_n\ \sin(n\theta)-b_n\ \cos(n\theta))\ <\ \frac{1}{n} \tag{A43}$$

□

Theorem 6.1.1

For the 3D modified Laplacian, any deformation is allowed for the radial solution if the deformation direction is in the angular direction. If the deformation is in the radial direction, then the maximum allowable deformation for the radial solution is

$$a_0\ <\ \begin{cases} \dfrac{R^{q+1}-1}{(q+1)R^{q+1}} & \text{if } q>-1 \\ \log(R) & \text{if } q=-1 \\ \dfrac{R^{|q|-1}-1}{(|q|-1)} & \text{if } -2<q<-1 \\ R-1 & \text{if } q=-2 \\ \dfrac{R^{|q|-1}-1}{(|q|-1)R^{|q|-2}} & \text{if } q<-2 \end{cases} \tag{A44}$$

Proof
The gradient of the radial component is

$$\nabla d_0(r) = \begin{cases} \left(a_0 \dfrac{(q+1)R^{q+1}}{r^{q+2}(1-R^{q+1})}, 0 \right) & \text{if } q \neq -1 \\ \left(\dfrac{-a_0}{r \log(R)}, 0 \right) & \text{if } q = -1 \end{cases} \tag{A45}$$

If the deformation direction is in the angular direction, then the validity function is always 0, so that any amount of angular deformation is allowed.

If the deformation direction is the radial direction, then the validity function is

$$v_0(r) = \begin{cases} \dfrac{a_0(q+1)R^{q+1}}{r^{q+2}(1-R^{q+1})} & \text{if } q \neq -1 \\ \dfrac{-a_0}{r \log(R)} & \text{if } q = -1 \end{cases} \tag{A46}$$

If $q = -1$, then the validity function is a negative function that is monotonically increasing. In the interval of interest, its minimum value is at $r = 1$, and the maximum allowable deformation is $a_0 < \log(R)$.

If $q > -1$, then the validity function is again a negative function that is monotonically increasing, and its minimum value over the interval is at $r = 1$. Hence, the maximum allowable deformation is

$$a_0 < \frac{R^{q+1} - 1}{(q+1)R^{q+1}} \tag{A47}$$

which decreases with q at approximately a rate of $1/q$.

If $-2 < q < -1$, then the validity function can be rewritten as

$$v_n(r) = \frac{(-|q|+1)R}{r^{-|q|+2}(R^{|q|} - R)} \tag{A48}$$

which is negative and monotonically increasing, so that its minimum value and maximum allowable deformation are the same as for the case when $q > -1$, and the maximum allowable deformation is

$$a_0 = \frac{R^{|q|-1} - 1}{(1-|q|)} \tag{A49}$$

When $q < -2$, the validity function can be written as

$$v_n(r) = \frac{(-|q|+1)r^{|q|-2}R}{(R^{|q|} - R)} \tag{A50}$$

so it is a negative function that is decreasing. Hence, its minimum value is at $r = R$ and its maximum allowable deformation then is

$$a_0 < \frac{(R^{|q|-1} - 1)}{(|q|-1)R^{|q|-2}} \tag{A51}$$

For the case when $q=-2$, both restrictions for the maximum allowable deformation are equal and reduce to

$$a_0 = R - 1 \tag{A52}$$

which is the distance from the inner circle to the outer circle. □

Theorem 6.1.1a
For the 3D modified Laplacian with $q \geqslant -2$, when the deformation direction is purely radial, the maximum allowable deformation for the frequency solutions occurs at $r=1$. Under these circumstances, then the maximum allowable deformation is as follows:

$$|a_{mn}||T_m^n(\cos\theta)| < \frac{2(R^{\alpha_2}-1)}{\alpha_2(R^{\alpha_2}+1)+(q+1)(R^{\alpha_2}-1)} \tag{A53}$$

where $\alpha_2 = \sqrt{4n^2+q^2+4n+2q+1}$, $\varepsilon_3 = -q-1-\alpha_2/2$ and $\varepsilon_4 = -q-1+\alpha_2/2$.

Proof
The gradient of the frequency solution $d_{mn}(r,\theta,\phi)$ dotted into the radial direction is

$$a_{mn}\left(\frac{R^{\alpha_2}\varepsilon_3 r^{\varepsilon_3-1}-\varepsilon_4 r^{\varepsilon_4-1}}{R^{\alpha_2}-1}\right)T_n^m(\cos\theta)\mathrm{e}^{\mathrm{i}m\phi} \tag{A54}$$

where $\varepsilon_3 = -q-1-\alpha_2/2$ and $\varepsilon_4 = -q-1+\alpha_2/2$. The radial part is given by

$$\mathrm{Rad}_n(r) = \frac{R^{\alpha_2}\varepsilon_3 r^{\varepsilon_3-1}-\varepsilon_4 r^{\varepsilon_4-1}}{R^{\alpha_2}-1} \tag{A55}$$

Since $\varepsilon_3<0$ and $\varepsilon_4>0$ for all q and n, the radial part is negative for all positive values of r. As stated above, $\varepsilon_3<0$, so $\varepsilon_3-1<0$ for all q and n, so the behaviour of this first term in the numerator is the same for all values of q and n. However, since ε_4 can be greater or less than 1 based on the values of q and n, there are three cases: $n^2+n>q+2$, $n^2+n=q+2$ and $n^2+n<q+2$.

Case 1: $n^2+n>q+2$. In this case, $\varepsilon_4-1>0$, so the radial part is negative for all values of $r>0$ and approaches negative infinity as r approaches 0 and as r approach infinity. Thus, function has at least one extrema in the interval $(0,\infty)$. The extrema of the radial part are found by setting the derivative to zero and solving for r, which yields

$$r = R\left(\frac{\varepsilon_3(\varepsilon_3-1)}{\varepsilon_4(\varepsilon_4-1)}\right)^{1/\alpha_2} \tag{A56}$$

which shows that there is only one extrema in the interval $(0,\infty)$, which is a maximum. Thus, the minimum of the radial part on the interval $[1,R]$ must occur at the endpoints. At the endpoints, the radial part is

$$\frac{\partial \mathrm{Rad}_n}{\partial r}(1) = \frac{R^{\alpha_2}\varepsilon_3-\varepsilon_4}{R^{\alpha_2}-1}$$

$$\frac{\partial \mathrm{Rad}_n}{\partial r}(R) = \frac{R^{\alpha_2}\varepsilon_3 R^{\varepsilon_3 - 1} - \varepsilon_4 R^{\varepsilon_4 - 1}}{R^{\alpha_2} - 1} = \frac{(\varepsilon_3 - \varepsilon_4)R^{\varepsilon_4 - 1}}{R^{\alpha_2} - 1}$$

$$= -\frac{\alpha_2 R^{\varepsilon_4 - 1}}{R^{\alpha_2} - 1} \tag{A57}$$

To demonstrate when the value at $r = 1$ is more negative than the value at $r = R$, consider the following function of R:

$$\mathscr{F}(R) = R^{\alpha_2}\varepsilon_3 - \varepsilon_4 + \alpha_2 R^{\varepsilon_4 - 1} \tag{A58}$$

If $\mathscr{F} < 0$, then the value at $r = 1$ is greater than the value at $r = R$. Clearly, $\mathscr{F}(1) = 0$, and $\lim_{R\to\infty} \mathscr{F}(R) = -\infty$. If $\mathscr{F}$ has no critical points between 1 and ∞, then the functional is a negative, monotonically decreasing function for $R > 1$. To identify the critical points, set the derivative of $\mathscr{F}(R) = 0$, or

$$\mathscr{F}'(R) = \alpha_2 R^{\alpha_2 - 1}\varepsilon_3 + (\varepsilon_4 - 1)\alpha_2 R^{\varepsilon_4 - 2} = 0 \tag{A59}$$

Rearranging,

$$R^{\alpha_2 + 1 - \varepsilon_4} = \frac{1 - \varepsilon_4}{\varepsilon_3} \tag{A60}$$

The critical points of $\mathscr{F}(R)$ will be greater than 1, only if

$$\frac{1 - \varepsilon_4}{\varepsilon_3} > 1 \tag{A61}$$

which will occur whenever $q < -2$. Hence, when $q > -2$, the critical point of $\mathscr{F}(R)$ is less than one, so that $\mathscr{F}(R) < 0$ for all values of $R > 1$, and the radial part is more negative at $r = 1$ than at $r = R$. Thus, the maximum allowable deformation occurs at $r = 1$ and must satisfy

$$|a_{mn}||T_n^m(\cos\theta)| < \frac{2(R^{\alpha_2} - 1)}{\alpha_2(R^{\alpha_2} + 1) + (q + 1)(R^{\alpha_2} - 1)} \tag{A62}$$

Case 2: $n^2 + n = q + 2$. In this case, $\varepsilon_4 - 1 = 0$, so the radial part $\mathrm{Rad}_n(r)$ simplifies to

$$\mathrm{Rad}_n(r) = -\frac{R^{q+3}(q + 2)r^{-q-3} + 1}{R^{q+3} - 1} \tag{A63}$$

This function approaches $-\infty$ as r approaches 0 and approaches $-(1/R^{q+3} - 1)$ as r approaches ∞. It is a negative function for all positive values of r and is monotonically increasing with r. Hence, on the interval $[1, R]$, it is most restrictive at $r = 1$, and the same maximum allowable deformation applies.

Case 3: $n^2 + n < q + 2$. Following the derivation given above, since $n^2 + n < q + 2$, then $\varepsilon_4 - 1 < 0$. Under these circumstances, the radial part approaches negative infinity as r approaches 0 and approaches 0 as r approaches infinity. The critical points for the radial part satisfy the following equation:

$$r = R\left(\frac{\varepsilon_3(\varepsilon_3 - 1)}{\varepsilon_4(\varepsilon_4 - 1)}\right)^{1/\alpha_2} \tag{A64}$$

The fraction under the radical is negative, because $\varepsilon_3 < 0$ and $0 < \varepsilon_4 < 1$. Hence, there is no critical point for $r > 0$, the radial part is a negative monotonically increasing function of r, the most negative value occurs when $r = 1$, and the same restriction for the maximum allowable deformation holds. □

Theorem 6.1.2b

For the 3D modified Laplacian with $q < -2$, when the deformation direction is purely radial, the maximum allowable deformation for the frequency solutions occurs at $r = 1$, if the outer radius R satisfies $R^{\alpha_2}\varepsilon_3 + \alpha_2 R^{\varepsilon_4 - 1} < \varepsilon_4$, where $\varepsilon_3 = -q - 1 - \alpha_2/2$ and $\varepsilon_4 = -q - 1 + \alpha_2/2$. Under these circumstances, then the maximum allowable deformation is as follows:

$$|a_{mn}||T_m^n(\cos\theta)| < \frac{2(R^{\alpha_2} - 1)}{\alpha_2(R^{\alpha_2} + 1) + (q+1)(R^{\alpha_2} - 1)} \tag{A65}$$

Proof

Following the derivation given above, if $q < 0$, then the functional $\mathscr{F}(R)$ is positive for all R between 1 and $R_{\max}$. It is then negative for all values $R > R_{\max}$. If R satisfies the conditions of the theorem, then $\mathscr{F}(R) < 0$, and the radial part is more negative at $r = R$ than at $r = 1$.

Thus, under the conditions of the theorem, the maximum allowable deformation occurs at $r = 1$ and satisfies

$$|a_{mn}||T_m^n(\cos\theta)| < \frac{2(R^{\alpha_2} - 1)}{\alpha_2(R^{\alpha_2} + 1) + (q+1)(R^{\alpha_2} - 1)} \tag{A66}$$

□

REFERENCES

1. Lohner R, Yang C, Onate E. Viscous free surface hydrodynamics using unstructured grids. *Proceedings of 22nd Symposium on Naval Hydrodynamics*, August 1998.
2. Crumpton PI, Giles MB. Implicit time-accurate solutions on unstructured dynamic grids. *International Journal for Numerical Methods in Fluids* 1997; **25**(11):1285–1300.
3. Masud A, Hughes TJR. A space–time Galerkin/least-squares finite element formulation for the Navier–Stokes equations for moving domain problems. *Computer Methods in Applied Mechanics and Engineering* 1997; **146**:91–126.
4. Tezduyar TE, Behr M, Liou J. A new strategy for finite-element computations involving moving boundaries and interfaces—the deforming-spatial-domain/space–time procedure: I, the concept and the preliminary numerical tests. *Computer Methods in Applied Mechanics and Engineering* 1992; **94**:339–351.
5. Cavallo PA, Hosangadi A, Lee RA, Dash SM. Dynamic unstructured grid methodology with application to aero/propulsive flowfields. *AIAA Paper 97-2310*, 1997.
6. Nielson EJ, Anderson WK. Recent improvements in aerodynamic design optimization on unstructured meshes. *AIAA Journal* 2002; **40**(6):1155–1163.
7. Tezduyar TE, Behr M, Mittal M, Johnson AA. Computation of unsteady incompressible flows with the finite element methods—space–time formulations, iterative strategies and massively parallel implementations. In *New Methods in Transient Analysis*, AMD-vol. 143, Smolinski P, Liu WK, Hulbert G, Tamma K (eds). ASME: New York, 1992; 7–24.
8. Stein K, Tezduyar T, Benney R. Mesh moving techniques for fluid-structure interactions with large displacements. *Transactions of the ASME* 2003; **70**(1):58–63.
9. Batina JT, Unsteady Euler airfoil solutions using unstructured dynamics meshes. *AIAA Journal* 1990; **28**(8):1381–1388.
10. Anderson WK, Venkatakrishnan V. Aerodynamic design optimization on unstructured grids with a continuous adjoint formulation. *AIAA Paper 97-0643*, 1997.
11. Singh KP, Newman JC, Baysal O. Dynamic unstructured method for flows past multiple objects in relative motion. *AIAA Journal* 1995; **33**(4):641–649.

12. Zhang S, Belegundu AD. Self-adaptive grid method with application to airfoil flow. *AIAA Journal* 1987; **25**(4):1249–1254.
13. Samareh JA. Application of quaternions for mesh deformation. *NASA TM 2002-211646*, 2002.
14. Nakahashi K, Deiwert GS. Self-adaptive-grid method with application to airfoil flow. *AIAA Journal* 1987; **25**(4):513–520.
15. Farhat C, Degand C, Koobus B, Lesoinne M. Torsional springs for two-dimensional dynamic unstructured fluid meshes. *Computer Methods in Applied Mechanics and Engineering* 1998; **163**:231–245.
16. Degand C, Farhat C. A three-dimensional torsional spring analogy method for unstructured dynamic meshes. *Computers and Structures* 2002; **80**:305–316.
17. Murayama M, Nakahashi K, Matsushima K. Unstructured dynamic mesh for large movement and deformation. *AIAA Paper 2002-0122*, 2002.
18. Burg COE. A robust unstructured grid movement strategy using three-dimensional torsional springs. *AIAA Paper 2004-2529*, 2004.
19. Burg COE, Sreenivas K, Hyams D, Mitchell B. Unstructured nonlinear free surface solutions: validation and verification. *AIAA Paper 2002-2977*, 2002.
20. Burg COE, Sreenivas K, Hyams D, Mitchell B. Unstructured nonlinear free surface simulations for the fully-appended DTMB model 5415 series hull including rotating propulsors. *Proceedings of 24th Symposium on Naval Hydrodynamics*, Fukuoka, Japan, July 2002.
21. Blom FJ. Considerations on the spring analogy. *International Journal of Numerical Methods in Fluids* 2000; **32**(6):647–668.

